






Article

# Analytical Analysis of Fractional-Order Multi-Dimensional Dispersive Partial Differential Equations

Shuang-Shuang Zhou <sup>1,†</sup>, Mounirah Areshi <sup>2,†</sup>, Praveen Agarwal <sup>3,4,†</sup>, Nehad Ali Shah <sup>5,†</sup>,  
Jae Dong Chung <sup>5,†</sup> and Kamsing Nonlaopon <sup>6,\*,†</sup>

- <sup>1</sup> School of Science, Hunan City University, Yiyang 413000, China; zhoushuangshuang21@126.com or zhoushuangshuang@hncu.edu.cn  
<sup>2</sup> Mathematics Department, College of Science, University of Tabuk, Tabuk 71491, Saudi Arabia; m.areshi@ut.edu.sa  
<sup>3</sup> Department of Mathematics, Anand International College of Engineering, Jaipur 302022, India; goyal.praveen2011@gmail.com or praveen.agarwal@anandice.ac.in  
<sup>4</sup> Nonlinear Dynamics Research Center (NDRC), Ajman University, Ajman 346, United Arab Emirates  
<sup>5</sup> Department of Mechanical Engineering, Sejong University, Seoul 05006, Korea; nehadali199@yahoo.com (N.A.S.); jdchung@sejong.ac.kr (J.D.C.)  
<sup>6</sup> Department of Mathematics, Faculty of Science, Khon Kaen University, Khon Kaen 40002, Thailand  
\* Correspondence: nkamsi@kku.ac.th  
† These authors contributed equally to this work.

**Abstract:** In this paper, a novel technique called the Elzaki decomposition method has been using to solve fractional-order multi-dimensional dispersive partial differential equations. Elzaki decomposition method results for both integer and fractional orders are achieved in series form, providing a higher convergence rate to the suggested technique. Illustrative problems are defined to confirm the validity of the current technique. It is also researched that the conclusions of the fractional-order are convergent to an integer-order result. Moreover, the proposed method results are compared with the exact solution of the problems, which has confirmed that approximate solutions are convergent to the exact solution of each problem as the terms of the series increase. The accuracy of the method is examined with the help of some examples. It is shown that the proposed method is found to be reliable, efficient and easy to use for various related problems of applied science.

**Keywords:** Elzaki transform; Adomian decomposition method; multi-dimensional dispersive equations; Caputo derivatives



**Citation:** Zhou, S.-S.; Areshi, M.; Agarwal, P.; Shah, N.A.; Chung, J.D.; Nonlaopon, K. Analytical Analysis of Fractional-Order Multi-Dimensional Dispersive Partial Differential Equations. *Symmetry* **2021**, *13*, 939. <https://doi.org/10.3390/sym13060939>

Academic Editor: Calogero Vetro and Sun Young Cho

Received: 22 March 2021  
Accepted: 21 May 2021  
Published: 26 May 2021

**Publisher's Note:** MDPI stays neutral with regard to jurisdictional claims in published maps and institutional affiliations.



**Copyright:** © 2021 by the authors. Licensee MDPI, Basel, Switzerland. This article is an open access article distributed under the terms and conditions of the Creative Commons Attribution (CC BY) license (<https://creativecommons.org/licenses/by/4.0/>).

## 1. Introduction

At the end of the 17th century, the concept of fractional calculus was discussed. Systems with an arbitrary order have recently gotten a lot of attention and recognition as a generalization of the classical order system. The fractional calculus fundamental cornerstone was laid nearly 324 years ago, and it has proven deeply rooted mathematical principles since then. The scheme of integer and fractional-order differential equations can efficiently explain any real-world problem. In reality, such systems can be used in medicine, control theory, thermodynamics, biology, electronics, signal processing, and other fields [1,2]. The immediate and vital solutions connected to the results of fractional-order differential equations are shown in [3,4]. We can study changes in the neighborhood of a point using the integer-order derivative, but we can check changes in the entire interval using the fractional derivative. The models connecting to implementations of fractional calculus are presented in many branches of applied science such as continuum mechanics and fluid, chaos, electrodynamics, cosmology, optics, and many other units [5–7].

Fractional partial differential equations (FPDEs) are used in numerous applied physics fields, such as quantum mechanics, mathematical biology, fluid dynamics, chemical kinetics and linear optics, to model various physical phenomena. In 1895, the Korteweg–De Vries

(KdV) constructed a non-dimensionalized version of the equation known as the KdV equation. The scheme consisting of integer partial differential equations and fractional-order partial differential equations with the fractional Caputo derivative has a well-designed symmetry structure. This problem is utilized to analyze dispersive wave phenomena in different areas of applied science, like quantum mechanics and plasma physics. KdV's exact solution might not be available, so many analytical methods for its analytical result [8] have been discussed. There are two essential dispersive terms in KdV equations, respectively, third and fifth order. For the definition of plasma physics, the KdV equation of order five was used with [9]. Numerical results of the dispersive KdV equations of the third and fifth orders were investigated in [10].

The non-linear existence is important for the full analysis of any physical structure, demonstrating the value of the non-linear term present in any physical problem model. In this relation, the reductive disruption principle for non-linear KdV has been studied in [11]. The variational technique has been proposed in [12] for the exact KdV result with higher-order nonlinearity. The approximate result for the KdV–Burgers equation was successfully derived in [13] utilizing the compact form constrained interpolation profile technique. The computational results of KdV equations are described in [8] utilizing the homotopy perturbation transformation methodology. The KdV equations of fractional-order three and five have been used in [10] by utilized two approximate techniques. The homotopy analysis transform method can be analyzed to have solved FDEs [14], a new analytical technique for solving a system of nonlinear fractional partial differential equations [15]. Feng achieved non-linear coupled time-fractional modified KdV equations: first integral technique [16]. Fractional-order partial differential equations three have been used by different techniques, such as fractional-order variational iteration techniques [17], Riccati method [18], fractional differential transformation technique and modified fractional-order differential transformation technique [19], Spline technique [20] and Homotopy analysis transform technique [21].

G. Adomian is an American scientist who has developed the Adomian decomposition method. It focuses on searching for a set of solutions and on the decomposition of the non-linear operator into a sequence in which Adomian polynomials [22] are recurrently computed to use the terms. This method is improved with Elzaki transformation, such that the improved method is known as the Elzaki decomposition method (EDM). Elzaki Transform (ET) is a modern integral transform introduced by Tarig Elzaki in 2010. ET is a modified transform of Sumudu and Laplace transforms. It is important to note that there are many differential equations with variable coefficients that Sumudu and Laplace cannot accomplish transforms but can be conveniently done using ET [23–25]. Many mathematicians have been solving differential equations with the aid of ET, such as Navier–Stokes equations [26], heat-like equations [27], Fisher's equation and hyperbolic equation [28].

In this article, the Elzaki decomposition technique are applied of investigate the result of fractional-order multi-dimensional dispersive partial differential equations. The fractional derivatives are define by the Caputo operator. The result of the given problems is show that the validity of the suggested method. The solutions of the suggested technique are analyzed and shown with the help of table and figures. Applying the current method, the results of time-fractional equations as well as integral-order equations, are investigated. The given mehtod is very helpful in solving other fractional-order of PDEs.

The rest of this article is organized as follows. In Section 2, important definitions is presented. In Section 3 basic idea of Elzaki decomposition method are given. The approximate solutions and graphs for the achieved results are presented in Section 4. Finally, we give our conclusions in Section 5.

## 2. Preliminaries

**Definition 1.** The fractional Abel-Riemann operator  $D^\vartheta$  of order  $\vartheta$  is given as [23–25]

$$D^\vartheta v(\mathfrak{S}) = \begin{cases} \frac{d^j}{d\mathfrak{S}^j} v(\mathfrak{S}), & \vartheta = j \\ \frac{1}{\Gamma(j-\vartheta)} \frac{d}{d\mathfrak{S}} \int_0^{\mathfrak{S}} \frac{v(\psi)}{(\mathfrak{S}-\psi)^{\vartheta-j+1}} d\psi, & j-1 < \vartheta < j \end{cases}$$

where  $j \in \mathbb{Z}^+$ ,  $\vartheta \in \mathbb{R}^+$  and

$$D^{-\vartheta} v(\mathfrak{S}) = \frac{1}{\Gamma(\vartheta)} \int_0^{\mathfrak{S}} (\mathfrak{S}-\psi)^{\vartheta-1} v(\psi) d\psi, \quad 0 < \vartheta \leq 1.$$

**Definition 2.** The fractional-order Abel-Riemann integration operator  $J^\vartheta$  is defined as [23–25]

$$J^\vartheta v(\mathfrak{S}) = \frac{1}{\Gamma(\vartheta)} \int_0^{\mathfrak{S}} (\mathfrak{S}-\psi)^{\vartheta-1} v(\psi) d\mathfrak{S}, \quad \mathfrak{S} > 0, \quad \vartheta > 0.$$

The operator of basic properties:

$$\begin{aligned} J^\vartheta \mathfrak{S}^j &= \frac{\Gamma(j+1)}{\Gamma(j+\vartheta+1)} \mathfrak{S}^{j+\vartheta} \\ D^\vartheta \mathfrak{S}^j &= \frac{\Gamma(j+1)}{\Gamma(j-\vartheta+1)} \mathfrak{S}^{j-\vartheta} \end{aligned}$$

**Definition 3.** The Caputo fractional operator  $D^\vartheta$  of  $\vartheta$  is defined as [23–25]

$${}^C D^\vartheta v(\mathfrak{S}) = \begin{cases} \frac{1}{\Gamma(j-\vartheta)} \int_0^{\mathfrak{S}} \frac{v^j(\psi)}{(\mathfrak{S}-\psi)^{\vartheta-j+1}} d\psi, & j-1 < \vartheta < j, \\ \frac{d^j}{d\mathfrak{S}^j} v(\mathfrak{S}), & j = \vartheta. \end{cases} \quad (1)$$

## 3. The EDM Method, Applied to Two Equations

### 3.1. EDM for Fractional-Order One-Dimensional Dispersive Equation

In this section, EDM is used to solve fractional-order dispersive partial differential equation.

$$\frac{\partial^\vartheta \mu(\psi, \mathfrak{S})}{\partial \mathfrak{S}^\vartheta} + w \frac{\partial^3 \mu(\psi, \mathfrak{S})}{\partial \psi^3} = q(\psi, \mathfrak{S}), \quad w, \mathfrak{S} \geq 0, \quad \psi_0 < \psi < \psi_1, \quad 0 < \vartheta \leq 1, \quad (2)$$

where is  $D^\vartheta \mu = \frac{\partial^\vartheta \mu(\psi, \mathfrak{S})}{\partial \mathfrak{S}^\vartheta}$  the fractional-order Caputo operator of  $\vartheta$ ,  $w$  is constant,  $\frac{\partial^3 \mu(\psi, \mathfrak{S})}{\partial \psi^3}$  is linear function and the source term is  $q(\psi, \mathfrak{S})$ .

With the initial condition

$$\mu(\psi, 0) = k(\psi), \quad \psi_0 \leq \psi \leq \psi_1 \quad (3)$$

the boundary conditions are

$$\mu(0, \mathfrak{S}) = g_0(\mathfrak{S}), \quad \frac{\partial \mu(0, \mathfrak{S})}{\partial \psi} = g_1(\mathfrak{S}), \quad \frac{\partial^2 \mu(0, \mathfrak{S})}{\partial \psi^2} = g_2(\mathfrak{S}) \quad \mathfrak{S} > 0. \quad (4)$$

The  $k(\psi)$  are assumed to be continuous, the space interval  $\psi_0 \leq \psi \leq \psi_1$  will be divided into  $N$  sub intervals each of width  $h$  so that  $Nh = \psi_1 - \psi_0$ , and the time variable will be discretized in steps of length  $l$ .

Applying Elzaki transform to Equation (2), we get

$$E \left[ \frac{\partial^\vartheta \mu(\psi, \mathfrak{S})}{\partial \mathfrak{S}^\vartheta} \right] + E \left[ w \frac{\partial^3 \mu(\psi, \mathfrak{S})}{\partial \psi^3} \right] = E[q(\psi, \mathfrak{S})], \quad (5)$$

$$E[\mu(\psi, \mathfrak{S})] = k(x)s^2 + s^\theta E[q(\psi, \mathfrak{S})] - s^\theta E\left[w \frac{\partial^3 \mu(\psi, \mathfrak{S})}{\partial \psi^3}\right]. \tag{6}$$

The EDM result  $\mu(\psi, \mathfrak{S})$  is represent by the following infinite series

$$\mu(\psi, \mathfrak{S}) = \sum_{j=0}^{\infty} \mu_j(\psi, \mathfrak{S}), \tag{7}$$

and the non-linear terms of Adomian polynomials, is defined as

$$N\mu(\psi, \mathfrak{S}) = \sum_{j=0}^{\infty} A_j, \tag{8}$$

$$A_j = \frac{1}{j!} \left[ \frac{d^j}{d\lambda^j} \left\{ N \sum_{j=0}^{\infty} (\lambda^j \mu_j) \right\} \right]_{\lambda=0}, \quad j = 0, 1, 2 \dots \tag{9}$$

put Equations (6) and (7) in Equation (5), we get

$$E\left[\sum_{j=0}^{\infty} \mu(\psi, \mathfrak{S})\right] = k(x)s^2 + s^\theta E[q(\psi, \mathfrak{S})] - s^\theta E\left[w \frac{\partial^3 \mu_j(\psi, \mathfrak{S})}{\partial \psi^3}\right]. \tag{10}$$

Using the linearity properties of the Elzaki transformation,

$$E[\mu_0(\psi, \mathfrak{S})] = \mu(\psi, 0)s^2 + s^\theta E[q(\psi, \mathfrak{S})] = k(\psi, s),$$

$$E[\mu_1(\psi, \mathfrak{S})] = -s^\theta E\left[w \frac{\partial^3 \mu_0(\psi, \mathfrak{S})}{\partial \psi^3}\right].$$

Generally, we can write

$$E[\mu_{j+1}(\psi, \mathfrak{S})] = -s^\theta E\left[\frac{\partial^3 \mu_j(\psi, \mathfrak{S})}{\partial \psi^3}\right], \quad j \geq 1. \tag{11}$$

Applying the inverse Elzaki transform, in Equation (10)

$$\mu_0(\psi, \mathfrak{S}) = k(\psi, \mathfrak{S}),$$

$$\mu_{j+1}(\psi, \mathfrak{S}) = -E^{-1} \left[ s^\theta E \left\{ \frac{\partial^3 \mu_j(\psi, \mathfrak{S})}{\partial \psi^3} \right\} \right]. \tag{12}$$

### 3.2. EDM for Fractional Multi-Dimensional Dispersive Equation

The higher-dimension dispersive partial differential equation is define as,

$$\frac{\partial^\theta \mu}{\partial \mathfrak{S}^\theta} + c \frac{\partial^3 \mu}{\partial \psi^3} + d \frac{\partial^3 \mu}{\partial \phi^3} + e \frac{\partial^3 \mu}{\partial \varphi^3} = q(\psi, \phi, \varphi, \mathfrak{S}), \quad \mathfrak{S} \geq 0, \quad c, d, e \geq 0, \quad 0 < \theta < 1, \tag{13}$$

where the source term is define by  $q(\psi, \phi, \varphi, \mathfrak{S})$ .

With initial condition is

$$\mu(\psi, \phi, \varphi, 0) = k(\psi, \phi, \varphi). \tag{14}$$

Applying Elzaki transformation to Equation (13), we get

$$E\left[\frac{\partial^\theta \mu}{\partial \mathfrak{S}^\theta}\right] + E\left[c \frac{\partial^3 \mu}{\partial \psi^3} + d \frac{\partial^3 \mu}{\partial \phi^3} + e \frac{\partial^3 \mu}{\partial \varphi^3}\right] = E[q(\psi, \phi, \varphi, \mathfrak{S})], \tag{15}$$

$$E \left[ \sum_{j=0}^{\infty} \mu(\psi, \phi, \varphi, \mathfrak{S}) \right] = k(\psi, \phi, \varphi, z)s^2 + s^\theta E[q(\psi, \phi, \varphi, \mathfrak{S})] - s^\theta E \left[ c \frac{\partial^3 \mu}{\partial \psi^3} + d \frac{\partial^3 \mu}{\partial \phi^3} + e \frac{\partial^3 \mu}{\partial \varphi^3} \right]. \quad (16)$$

Applying the linearity of the Elzaki transform,

$$E[\mu_0(\psi, \phi, \varphi, \mathfrak{S})] = \mu(\psi, \phi, \varphi, 0)s^2 + s^\theta E[q(\psi, \phi, \varphi, \mathfrak{S})] = k(\psi, \phi, \varphi, s),$$

$$E[\mu_1(\psi, \phi, \varphi, \mathfrak{S})] = -s^\theta E \left[ c \frac{\partial^3 \mu_0}{\partial \psi^3} + d \frac{\partial^3 \mu_0}{\partial \phi^3} + e \frac{\partial^3 \mu_0}{\partial \varphi^3} \right].$$

Generally, we can write

$$E[\mu_{j+1}(\psi, \phi, \varphi, \mathfrak{S})] = -s^\theta E \left[ c \frac{\partial^3 \mu_j}{\partial \psi^3} + d \frac{\partial^3 \mu_j}{\partial \phi^3} + e \frac{\partial^3 \mu_j}{\partial \varphi^3} \right], \quad j \geq 1. \quad (17)$$

Applying the inverse Elzaki transform of Equation (16)

$$\mu_0(\psi, \phi, \varphi, \mathfrak{S}) = k(\psi, \phi, \varphi, \mathfrak{S}),$$

$$\mu_{j+1}(\psi, \phi, \varphi, \mathfrak{S}) = -E^{-1} \left[ s^\theta E \left\{ c \frac{\partial^3 \mu_j}{\partial \psi^3} + d \frac{\partial^3 \mu_j}{\partial \phi^3} + e \frac{\partial^3 \mu_j}{\partial \varphi^3} \right\} \right]. \quad (18)$$

#### 4. Results

**Example 1.** Consider the following fractional-order dispersive KdV equation [29]

$$\frac{\partial^\theta \mu}{\partial \mathfrak{S}^\theta} + 2 \frac{\partial \mu}{\partial \psi} + \frac{\partial^3 \mu}{\partial \psi^3} = 0, \quad \mathfrak{S} > 0, \quad 0 < \theta \leq 1, \quad (19)$$

with initial condition

$$\mu(\psi, 0) = \sin \psi, \quad (20)$$

using Elzaki transformation of (19), we get

$$E \left[ \frac{\partial^\theta \mu}{\partial \mathfrak{S}^\theta} \right] = -E \left[ 2 \frac{\partial \mu}{\partial \psi} + \frac{\partial^3 \mu}{\partial \psi^3} \right],$$

$$\frac{1}{s^\theta} E[\mu(\psi, \mathfrak{S})] - s^{2-\theta} [\mu(\psi, 0)] = -E \left[ 2 \frac{\partial \mu}{\partial \psi} + \frac{\partial^3 \mu}{\partial \psi^3} \right].$$

Applying inverse Elzaki transform

$$\mu(\psi, \mathfrak{S}) = E^{-1} \left[ s^2 \mu(\psi, 0) - s^\theta E \left\{ 2 \frac{\partial \mu}{\partial \psi} + \frac{\partial^3 \mu}{\partial \psi^3} \right\} \right],$$

$$\mu(\psi, \mathfrak{S}) = \sin \psi - E^{-1} \left[ s^\theta E \left\{ 2 \frac{\partial \mu}{\partial \psi} + \frac{\partial^3 \mu}{\partial \psi^3} \right\} \right].$$

Using ADM procedure, we get

$$\sum_{j=0}^{\infty} \mu_j(\psi, \mathfrak{S}) = \sin \psi - E^{-1} \left[ s^\theta E \left\{ 2 \sum_{j=0}^{\infty} \frac{\partial \mu_j}{\partial \psi} + \sum_{j=0}^{\infty} \frac{\partial^3 \mu_j}{\partial \psi^3} \right\} \right],$$

$$\mu_0(\psi, \mathfrak{S}) = \sin \psi, \quad (21)$$

$$\mu_{j+1}(\psi, \mathfrak{S}) = -E^{-1} \left[ s^\theta E \left\{ 2 \sum_{j=0}^{\infty} \frac{\partial \mu_j}{\partial \psi} + \sum_{j=0}^{\infty} \frac{\partial^3 \mu_j}{\partial \psi^3} \right\} \right],$$

for  $j = 0, 1, 2, \dots$

$$\begin{aligned}\mu_1(\psi, \mathfrak{S}) &= -E^{-1} \left[ s^\vartheta E \left\{ 2 \frac{\partial \mu_0}{\partial \psi} + \frac{\partial^3 \mu_0}{\partial \psi^3} \right\} \right] = -\cos \psi \frac{\mathfrak{S}^\vartheta}{\Gamma(\vartheta + 1)}, \\ \mu_2(\psi, \mathfrak{S}) &= -E^{-1} \left[ s^\vartheta E \left\{ 2 \frac{\partial \mu_1}{\partial \psi} + \frac{\partial^3 \mu_1}{\partial \psi^3} \right\} \right] = -\sin \psi \frac{\mathfrak{S}^{2\vartheta}}{\Gamma(2\vartheta + 1)}.\end{aligned}\quad (22)$$

The subsequent terms are

$$\mu_3(\psi, \mathfrak{S}) = -E^{-1} \left[ s^\vartheta E \left\{ 2 \frac{\partial \mu_2}{\partial \psi} + \frac{\partial^3 \mu_2}{\partial \psi^3} \right\} \right] = \cos \psi \frac{\mathfrak{S}^{3\vartheta}}{\Gamma(3\vartheta + 1)}.\quad (23)$$

The EDM solution for Example 1 is

$$\mu(\psi, \mathfrak{S}) = \mu_0(\psi, \mathfrak{S}) + \mu_1(\psi, \mathfrak{S}) + \mu_2(\psi, \mathfrak{S}) + \mu_3(\psi, \mathfrak{S}) + \dots$$

$$\mu(\psi, \mathfrak{S}) = \sin \psi - \cos \psi \frac{\mathfrak{S}^\vartheta}{\Gamma(\vartheta + 1)} - \sin \psi \frac{\mathfrak{S}^{2\vartheta}}{\Gamma(2\vartheta + 1)} + \cos \psi \frac{\mathfrak{S}^{3\vartheta}}{\Gamma(3\vartheta + 1)} + \dots$$

The solution for the series form is provided by

$$\begin{aligned}\mu(\psi, \mathfrak{S}) &= \sin \psi \left( 1 - \frac{\mathfrak{S}^{2\vartheta}}{\Gamma(2\vartheta + 1)} + \frac{\mathfrak{S}^{4\vartheta}}{\Gamma(4\vartheta + 1)} - \dots \right) \\ &\quad - \cos \psi \left( \frac{\mathfrak{S}^\vartheta}{\Gamma(\vartheta + 1)} - \frac{\mathfrak{S}^{3\vartheta}}{\Gamma(3\vartheta + 1)} + \frac{\mathfrak{S}^{5\vartheta}}{\Gamma(5\vartheta + 1)} - \dots \right),\end{aligned}\quad (24)$$

when  $\vartheta = 1$ , then EDM solution is

$$\mu(\psi, \mathfrak{S}) = \sin(\psi - \mathfrak{S}).\quad (25)$$

Figure 1 consists of two plots the exact and EDM results of  $\mu(\psi, \mathfrak{S})$  of Example 1 at  $\vartheta = 1$ . Both the graphs of Figure 1 indicate that the current technique has close contact with the exact result for the given. In Figure 2, two plots are given that represent the approximate result of Example 1 at fractional  $\vartheta = 0.8$  and  $0.6$ , respectively. Show that the solution surfaces of the fractional-order are convergent to the integer-order surface as the fractional-order approaches to the integer-order. It suggests that through the physical phenomena happening in nature, we can model any of the surfaces as desire physically.

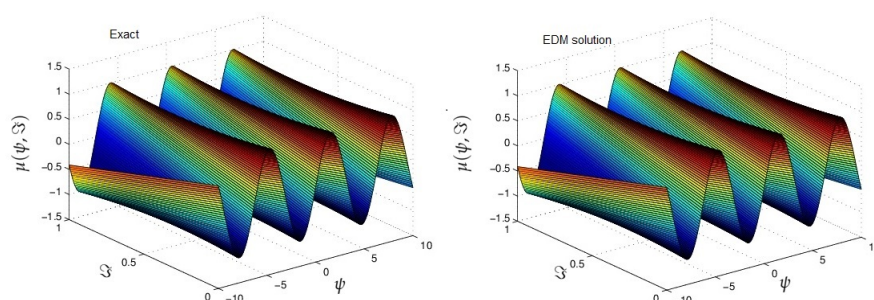
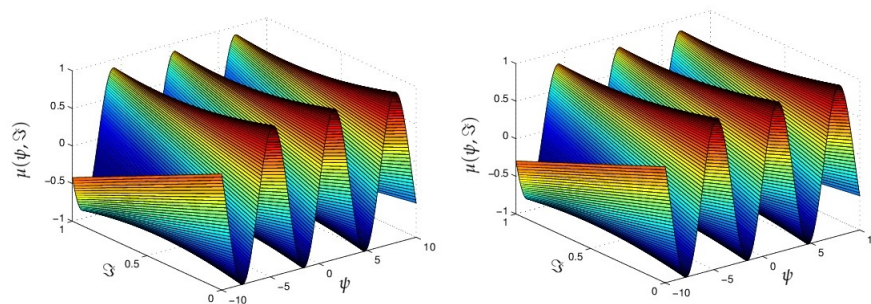


Figure 1. The graph of Exact and EDM solutions of  $\vartheta = 1$  of Example 1.



**Figure 2.** The graphs of different fractional-order  $\vartheta = 0.8$  and  $0.6$  of Example 1.

**Example 2.** Consider the fractional-order dispersive KdV equation [29]

$$\frac{\partial^\vartheta \mu}{\partial \mathfrak{S}^\vartheta} + \frac{\partial^3 \mu}{\partial \psi^3} + \frac{\partial^3 \mu}{\partial \phi^3} = 0, \quad \mathfrak{S} > 0, \quad 0 < \vartheta \leq 1, \quad (26)$$

the initial condition is

$$\mu(\psi, \phi, 0) = \cos(\psi + \phi). \quad (27)$$

Applying Elzaki transformation of (26), we get

$$E \left[ \frac{\partial^\vartheta \mu}{\partial \mathfrak{S}^\vartheta} \right] = -E \left[ \frac{\partial^3 \mu}{\partial \psi^3} + \frac{\partial^3 \mu}{\partial \phi^3} \right],$$

$$\frac{1}{s^\vartheta} E[\mu(\psi, \phi, \mathfrak{S})] - s^{2-\vartheta} [\mu(\psi, \phi, 0)] = -E \left[ \frac{\partial^3 \mu}{\partial \psi^3} + \frac{\partial^3 \mu}{\partial \phi^3} \right].$$

Using inverse Elzaki transformation,

$$\mu(\psi, \phi, \mathfrak{S}) = E^{-1} \left[ s^2 \mu(\psi, \phi, 0) - s^\vartheta E \left\{ \frac{\partial^3 \mu}{\partial \psi^3} + \frac{\partial^3 \mu}{\partial \phi^3} \right\} \right],$$

$$\mu(\psi, \phi, \mathfrak{S}) = \cos(\psi + \phi) - E^{-1} \left[ s^\vartheta E \left\{ \frac{\partial^3 \mu}{\partial \psi^3} + \frac{\partial^3 \mu}{\partial \phi^3} \right\} \right].$$

Implemented the Adomian decomposition technique, we have

$$\sum_{j=0}^{\infty} \mu_j(\psi, \phi, \mathfrak{S}) = \cos(\psi + \phi) - E^{-1} \left[ s^\vartheta E \left\{ \sum_{j=0}^{\infty} \frac{\partial^3 \mu_j}{\partial \psi^3} + \sum_{j=0}^{\infty} \frac{\partial^3 \mu_j}{\partial \phi^3} \right\} \right],$$

$$\mu_0(\psi, \phi, \mathfrak{S}) = \cos(\psi + \phi), \quad (28)$$

$$\mu_{j+1}(\psi, \phi, \mathfrak{S}) = -E^{-1} \left[ s^\vartheta E \left\{ \sum_{j=0}^{\infty} \frac{\partial^3 \mu_j}{\partial \psi^3} + \sum_{j=0}^{\infty} \frac{\partial^3 \mu_j}{\partial \phi^3} \right\} \right],$$

for  $j = 0, 1, 2, \dots$

$$\mu_1(\psi, \phi, \mathfrak{S}) = -E^{-1} \left[ s^\vartheta E \left\{ \frac{\partial^3 \mu_0}{\partial \psi^3} + \frac{\partial^3 \mu_0}{\partial \phi^3} \right\} \right] = -2 \sin(\psi + \phi) \frac{\mathfrak{S}^\vartheta}{\Gamma(\vartheta + 1)}, \quad (29)$$

$$\mu_2(\psi, \phi, \mathfrak{S}) = -E^{-1} \left[ s^\vartheta E \left\{ \frac{\partial^3 \mu_1}{\partial \psi^3} + \frac{\partial^3 \mu_1}{\partial \phi^3} \right\} \right] = -4 \cos(\psi + \phi) \frac{\mathfrak{S}^{2\vartheta}}{\Gamma(2\vartheta + 1)}.$$

The subsequent terms are

$$\mu_3(\psi, \phi, \mathfrak{S}) = -E^{-1} \left[ s^\vartheta E \left\{ \frac{\partial^3 \mu_2}{\partial \psi^3} + \frac{\partial^3 \mu_2}{\partial \phi^3} \right\} \right] = 8 \sin(\psi + \phi) \frac{\mathfrak{S}^{3\vartheta}}{\Gamma(3\vartheta + 1)}. \quad (30)$$

The EDM solution for Example 2 is

$$\begin{aligned} \mu(\psi, \phi, \mathfrak{S}) &= \mu_0(\psi, \phi, \mathfrak{S}) + \mu_1(\psi, \phi, \mathfrak{S}) + \mu_2(\psi, \phi, \mathfrak{S}) + \mu_3(\psi, \phi, \mathfrak{S}), \dots, \\ \mu(\psi, \phi, \mathfrak{S}) &= \cos(\psi + \phi) - 2 \sin(\psi + \phi) \frac{\mathfrak{S}^\vartheta}{\Gamma(\vartheta + 1)} - 4 \cos(\psi + \phi) \frac{\mathfrak{S}^{2\vartheta}}{\Gamma(2\vartheta + 1)} \\ &\quad + 8 \sin(\psi + \phi) \frac{\mathfrak{S}^{3\vartheta}}{\Gamma(3\vartheta + 1)} + \dots, \end{aligned}$$

The series form solution is given by

$$\begin{aligned} \mu(\psi, \phi, \mathfrak{S}) &= \cos(\psi + \phi) \left( 1 - \frac{4\mathfrak{S}^{2\vartheta}}{\Gamma(2\vartheta + 1)} + \frac{16\mathfrak{S}^{2\vartheta}}{\Gamma(2\vartheta + 1)} - \dots \right) \\ &\quad - \sin(\psi + \phi) \left( \frac{2\mathfrak{S}^\vartheta}{\Gamma(\vartheta + 1)} - \frac{8\mathfrak{S}^{3\vartheta}}{\Gamma(3\vartheta + 1)} + \frac{32\mathfrak{S}^{5\vartheta}}{\Gamma(5\vartheta + 1)} - \dots \right), \end{aligned} \tag{31}$$

when  $\vartheta = 1$ , then EDM solution is

$$\mu(\psi, \phi, \mathfrak{S}) = \cos(\psi + \phi + 2\mathfrak{S}). \tag{32}$$

Figure 3 consists of two plots the exact and EDM results of  $\mu(\psi, \mathfrak{S})$  of Example 2 at  $\vartheta = 1$ . Both the graphs of Figure 3 indicate that the current technique has close contact with the exact result for the given. In Figure 4, two plots are given, that represents the approximate result of Example 2 at fractional  $\vartheta = 0.8$  and  $0.6$ , respectively. Figure 4 shows that the solution surfaces of the fractional-order are convergent to the integer-order surface as the fractional-order approaches to the integer-order. It suggests that through the physical phenomena happening in nature, we can model any of the surfaces as desire physically.

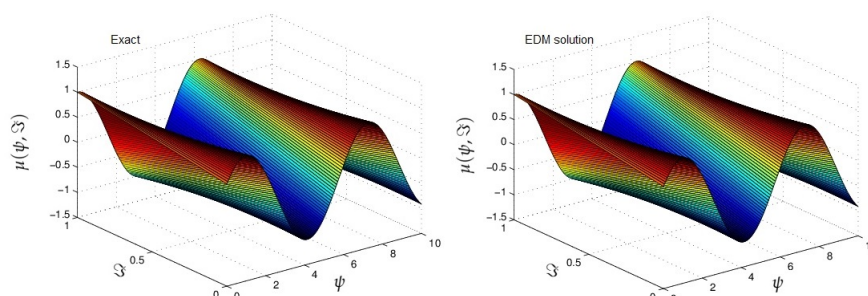


Figure 3. The graph of Exact and EDM solutions of  $\vartheta = 1$  of Example 2.

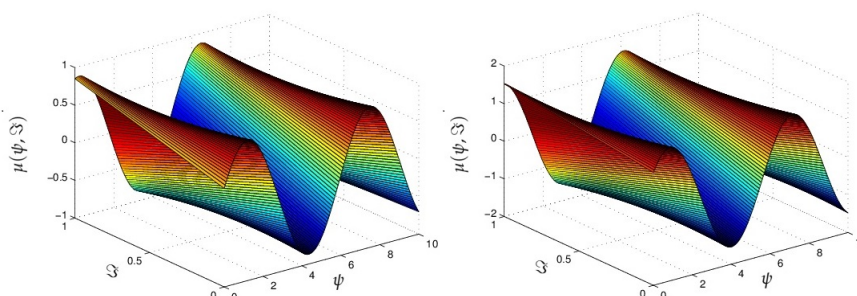


Figure 4. The graphs of different fractional-order  $\vartheta = 0.8$  and  $0.6$  of Example 2.

**Example 3.** Consider the fractional-order nonhomogeneous dispersive KdV equation [29]

$$\frac{\partial^\vartheta \mu}{\partial \mathfrak{S}^\vartheta} + \frac{\partial^3 \mu}{\partial \psi^3} = -\sin \pi \psi \sin \mathfrak{S} - \pi^3 \cos \pi \psi \cos \mathfrak{S}, \quad 0 < \vartheta \leq 1, \tag{33}$$



with initial condition

$$\mu(\psi, 0) = \sin \pi\psi, \quad (34)$$

using Elzaki transformation of (33), we get

$$E \left[ \frac{\partial^\theta \mu}{\partial \mathfrak{S}^\theta} \right] = E \left[ -\sin \pi\psi \sin \mathfrak{S} - \pi^3 \cos \pi\psi \cos \mathfrak{S} \right] - E \left[ \frac{\partial^3 \mu}{\partial \psi^3} \right],$$

$$\frac{1}{s^\theta} E[\mu(\psi, \mathfrak{S})] - s^{2-\theta} [\mu(\psi, 0)] = E \left[ -\sin \pi\psi \sin \mathfrak{S} - \pi^3 \cos \pi\psi \cos \mathfrak{S} \right] - E \left[ \frac{\partial^3 \mu}{\partial \psi^3} \right].$$

Applying inverse Elzaki transform

$$\mu(\psi, \mathfrak{S}) = E^{-1} \left[ s^2 \mu(\psi, 0) + s^\theta E \left\{ -\sin \pi\psi \sin \mathfrak{S} - \pi^3 \cos \pi\psi \cos \mathfrak{S} \right\} - s^\theta E \left\{ \frac{\partial^3 \mu}{\partial \psi^3} \right\} \right],$$

$$\mu(\psi, \mathfrak{S}) = E^{-1} \left[ s^2 \sin \pi\psi \right] + E^{-1} \left[ s^\theta E \left\{ -\sin \pi\psi \sin \mathfrak{S} - \pi^3 \cos \pi\psi \cos \mathfrak{S} \right\} \right] - E^{-1} \left[ s^\theta E \left\{ \frac{\partial^3 \mu}{\partial \psi^3} \right\} \right].$$

Implemented the Adomian decomposition technique, we have

$$\begin{aligned} \sum_{j=0}^{\infty} \mu_j(\psi, \mathfrak{S}) &= E^{-1} \left[ s^2 \sin \pi\psi \right] + E^{-1} \left[ s^\theta E \left\{ -\sin \pi\psi \left( \mathfrak{S} - \frac{\mathfrak{S}^3}{3!} + \frac{\mathfrak{S}^5}{5!} - \frac{\mathfrak{S}^7}{7!} + \frac{\mathfrak{S}^9}{9!} \right) \right\} \right] \\ &+ E^{-1} \left[ s^\theta E \left\{ -\pi^3 \cos \pi\psi \left( 1 - \frac{\mathfrak{S}^2}{2!} + \frac{\mathfrak{S}^4}{4!} - \frac{\mathfrak{S}^6}{6!} + \frac{\mathfrak{S}^8}{8!} \right) \right\} \right] - E^{-1} \left[ s^\theta E \left\{ \sum_{j=0}^{\infty} \frac{\partial^3 \mu_j}{\partial \psi^3} \right\} \right], \\ \mu_0(\psi, \mathfrak{S}) &= \sin \pi\psi - \sin \pi\psi \left( \frac{\mathfrak{S}^{\theta+1}}{\Gamma(\theta+2)} - \frac{\mathfrak{S}^{\theta+3}}{\Gamma(\theta+4)} + \frac{\mathfrak{S}^{\theta+5}}{\Gamma(\theta+6)} - \frac{\mathfrak{S}^{\theta+7}}{\Gamma(\theta+8)} + \frac{\mathfrak{S}^{\theta+9}}{\Gamma(\theta+10)} \right) \\ &- \pi^3 \cos \pi\psi \left( \frac{\mathfrak{S}^\theta}{\Gamma(\theta+1)} - \frac{\mathfrak{S}^{\theta+2}}{\Gamma(\theta+3)} + \frac{\mathfrak{S}^{\theta+4}}{\Gamma(\theta+5)} - \frac{\mathfrak{S}^{\theta+6}}{\Gamma(\theta+7)} + \frac{\mathfrak{S}^{\theta+8}}{\Gamma(\theta+9)} \right), \\ \mu_{j+1}(\psi, \mathfrak{S}) &= -E^{-1} \left[ s^\theta E \left\{ \sum_{j=0}^{\infty} \frac{\partial^3 \mu_j}{\partial \psi^3} \right\} \right], \end{aligned} \quad (35)$$

for  $j = 0, 1, 2, \dots$

$$\begin{aligned} \mu_1(\psi, \mathfrak{S}) &= -E^{-1} \left[ s^\theta E \left\{ \frac{\partial^3 \mu_0}{\partial \psi^3} \right\} \right], \\ \mu_1(\psi, \mathfrak{S}) &= \pi^3 \cos \pi\psi \frac{\mathfrak{S}^\theta}{\Gamma(\theta+1)} - \pi^3 \cos \pi\psi \left( \frac{\mathfrak{S}^{2\theta+1}}{\Gamma(2\theta+2)} - \frac{\mathfrak{S}^{2\theta+3}}{\Gamma(2\theta+4)} + \frac{\mathfrak{S}^{2\theta+5}}{\Gamma(2\theta+6)} \right. \\ &- \frac{\mathfrak{S}^{2\theta+7}}{\Gamma(2\theta+8)} + \frac{\mathfrak{S}^{2\theta+9}}{\Gamma(2\theta+10)} \left. \right) + \pi^6 \sin \pi\psi \left( \frac{\mathfrak{S}^{2\theta}}{\Gamma(2\theta+1)} - \frac{\mathfrak{S}^{2\theta+2}}{\Gamma(2\theta+3)} + \frac{\mathfrak{S}^{2\theta+4}}{\Gamma(2\theta+5)} \right. \\ &- \frac{\mathfrak{S}^{2\theta+6}}{\Gamma(2\theta+7)} + \frac{\mathfrak{S}^{2\theta+8}}{\Gamma(2\theta+9)} \left. \right), \\ \mu_2(\psi, \mathfrak{S}) &= -E^{-1} \left[ s^\theta E \left\{ \frac{\partial^3 \mu_1}{\partial \psi^3} \right\} \right], \\ \mu_2(\psi, \mathfrak{S}) &= -\pi^6 \sin \pi\psi \frac{\mathfrak{S}^{2\theta}}{\Gamma(2\theta+1)} + \pi^6 \sin \pi\psi \left( \frac{\mathfrak{S}^{3\theta+1}}{\Gamma(3\theta+2)} - \frac{\mathfrak{S}^{3\theta+3}}{\Gamma(3\theta+4)} + \frac{\mathfrak{S}^{3\theta+5}}{\Gamma(3\theta+6)} \right. \\ &- \frac{\mathfrak{S}^{3\theta+7}}{\Gamma(3\theta+8)} + \frac{\mathfrak{S}^{3\theta+9}}{\Gamma(3\theta+10)} \left. \right) + \pi^9 \cos \pi\psi \left( \frac{\mathfrak{S}^{3\theta}}{\Gamma(3\theta+1)} - \frac{\mathfrak{S}^{3\theta+2}}{\Gamma(3\theta+3)} + \frac{\mathfrak{S}^{3\theta+4}}{\Gamma(3\theta+5)} \right. \\ &- \frac{\mathfrak{S}^{3\theta+6}}{\Gamma(3\theta+7)} + \frac{\mathfrak{S}^{3\theta+8}}{\Gamma(3\theta+9)} \left. \right), \end{aligned} \quad (36)$$

The EDM solution for Example 3 is

$$\mu(\psi, \mathfrak{S}) = \mu_0(\psi, \mathfrak{S}) + \mu_1(\psi, \mathfrak{S}) + \mu_2(\psi, \mathfrak{S}) + \mu_3(\psi, \mathfrak{S}) + \dots,$$

$$\begin{aligned} \mu(\psi, \mathfrak{S}) = & \sin \pi \psi - \sin \pi \psi \left( \frac{\mathfrak{S}^{\vartheta+1}}{\Gamma(\vartheta+2)} - \frac{\mathfrak{S}^{\vartheta+3}}{\Gamma(\vartheta+4)} + \frac{\mathfrak{S}^{\vartheta+5}}{\Gamma(\vartheta+6)} - \frac{\mathfrak{S}^{\vartheta+7}}{\Gamma(\vartheta+8)} + \frac{\mathfrak{S}^{\vartheta+9}}{\Gamma(\vartheta+10)} \right) \\ & - \pi^3 \cos \pi \psi \left( \frac{\mathfrak{S}^{\vartheta}}{\Gamma(\vartheta+1)} - \frac{\mathfrak{S}^{\vartheta+2}}{\Gamma(\vartheta+3)} + \frac{\mathfrak{S}^{\vartheta+4}}{\Gamma(\vartheta+5)} - \frac{\mathfrak{S}^{\vartheta+6}}{\Gamma(\vartheta+7)} + \frac{\mathfrak{S}^{\vartheta+8}}{\Gamma(\vartheta+9)} \right) \\ & + \pi^3 \cos \pi \psi \frac{\mathfrak{S}^{\vartheta}}{\Gamma(\vartheta+1)} - \pi^3 \cos \pi \psi \left( \frac{\mathfrak{S}^{2\vartheta+1}}{\Gamma(2\vartheta+2)} - \frac{\mathfrak{S}^{2\vartheta+3}}{\Gamma(2\vartheta+4)} + \frac{\mathfrak{S}^{2\vartheta+5}}{\Gamma(2\vartheta+6)} - \frac{\mathfrak{S}^{2\vartheta+7}}{\Gamma(2\vartheta+8)} \right. \\ & \left. + \frac{\mathfrak{S}^{2\vartheta+9}}{\Gamma(2\vartheta+10)} \right) + \pi^6 \sin \pi \psi \left( \frac{\mathfrak{S}^{2\vartheta}}{\Gamma(2\vartheta+1)} - \frac{\mathfrak{S}^{2\vartheta+2}}{\Gamma(2\vartheta+3)} + \frac{\mathfrak{S}^{2\vartheta+4}}{\Gamma(2\vartheta+5)} - \frac{\mathfrak{S}^{2\vartheta+6}}{\Gamma(2\vartheta+7)} + \frac{\mathfrak{S}^{2\vartheta+8}}{\Gamma(2\vartheta+9)} \right) \\ & - \pi^6 \sin \pi \psi \frac{\mathfrak{S}^{2\vartheta}}{\Gamma(2\vartheta+1)} + \pi^6 \sin \pi \psi \left( \frac{\mathfrak{S}^{3\vartheta+1}}{\Gamma(3\vartheta+2)} - \frac{\mathfrak{S}^{3\vartheta+3}}{\Gamma(3\vartheta+4)} + \frac{\mathfrak{S}^{3\vartheta+5}}{\Gamma(3\vartheta+6)} - \frac{\mathfrak{S}^{3\vartheta+7}}{\Gamma(3\vartheta+8)} \right. \\ & \left. + \frac{\mathfrak{S}^{3\vartheta+9}}{\Gamma(3\vartheta+10)} \right) + \pi^9 \cos \pi \psi \left( \frac{\mathfrak{S}^{3\vartheta}}{\Gamma(3\vartheta+1)} - \frac{\mathfrak{S}^{3\vartheta+2}}{\Gamma(3\vartheta+3)} + \frac{\mathfrak{S}^{3\vartheta+4}}{\Gamma(3\vartheta+5)} - \frac{\mathfrak{S}^{3\vartheta+6}}{\Gamma(3\vartheta+7)} + \frac{\mathfrak{S}^{3\vartheta+8}}{\Gamma(3\vartheta+9)} \right) \\ & + \dots \end{aligned}$$

when  $\vartheta = 1$ , then EDM solution is

$$\mu(\psi, \mathfrak{S}) = \sin \pi \psi \cos \mathfrak{S}. \tag{37}$$

Figure 5 consists of two plots the exact and EDM results of  $\mu(\psi, \mathfrak{S})$  of Example 3 at  $\vartheta = 1$ . Both the graphs of Figure 5 indicate that the current technique has close contact with the exact result for the given. In Figure 6, two plots are given that represents the approximate result of Example 3 at fractional  $\vartheta = 0.8$  and  $0.6$ , respectively. Figure 6 shows that the solution surfaces of the fractional-order are convergent to the integer-order surface as the fractional-order approaches to the integer-order. It suggests that through the physical phenomena happening in nature, we can model any of the surfaces as desire physically.

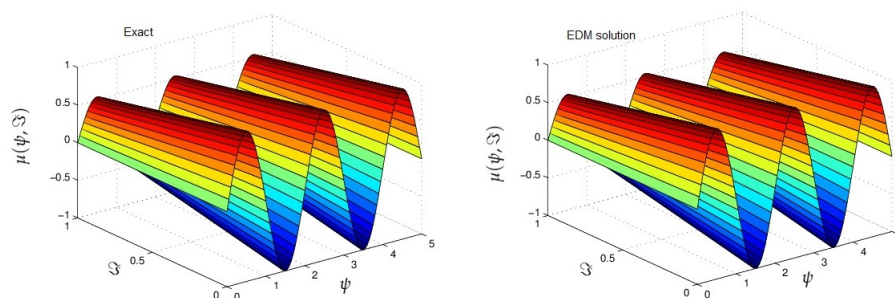


Figure 5. The graph of Exact and EDM solutions of  $\vartheta = 1$  of Example 3.

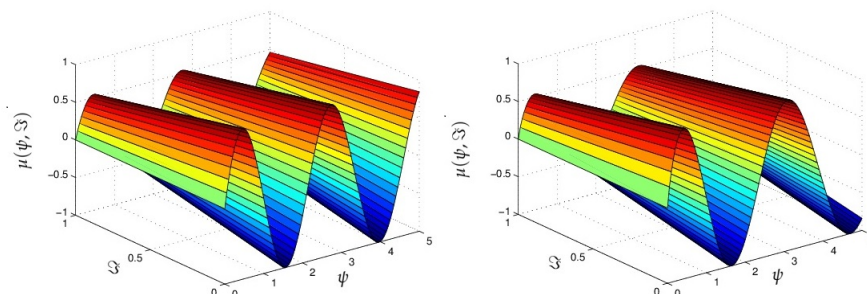


Figure 6. The graphs of different fractional-order  $\vartheta = 0.8$  and  $0.6$  of Example 3.

**Example 4.** Consider the fractional-order three dimensional nonhomogeneous dispersive KdV equation [29]

$$\frac{\partial^\theta \mu}{\partial \mathfrak{S}^\theta} + \frac{\partial^3 \mu}{\partial \psi^3} + \frac{1}{8} \frac{\partial^3 \mu}{\partial \phi^3} + \frac{1}{27} \frac{\partial^3 \mu}{\partial \varphi^3} = -\sin(\psi + 2\phi + 3\varphi) \cos \mathfrak{S} + \sin(\psi + 2\phi + 3\varphi) \cos \mathfrak{S}, \quad \mathfrak{S} > 0, \quad 0 < \theta \leq 1, \tag{38}$$

the initial condition is

$$\mu(\psi, \phi, \varphi, 0) = 0, \tag{39}$$

using Elzaki transform of (38), we get

$$\begin{aligned} E\left[\frac{\partial^\theta \mu}{\partial \mathfrak{S}^\theta}\right] &= E[\sin(\psi + 2\phi + 3\varphi) \cos \mathfrak{S}] - E[3 \cos(\psi + 2\phi + 3\varphi) \sin \mathfrak{S}] \\ &- E\left[\frac{\partial^3 \mu}{\partial \psi^3} + \frac{1}{8} \frac{\partial^3 \mu}{\partial \phi^3} + \frac{1}{27} \frac{\partial^3 \mu}{\partial \varphi^3}\right], \\ \frac{1}{s^\theta} E[\mu(\psi, \phi, \varphi, \mathfrak{S})] - s^{2-\theta} [\mu(\psi, \phi, \varphi, 0)] &= E[\sin(\psi + 2\phi + 3\varphi) \cos \mathfrak{S}] \\ &- E[3 \cos(\psi + 2\phi + 3\varphi) \sin \mathfrak{S}] - E\left[\frac{\partial^3 \mu}{\partial \psi^3} + \frac{1}{8} \frac{\partial^3 \mu}{\partial \phi^3} + \frac{1}{27} \frac{\partial^3 \mu}{\partial \varphi^3}\right]. \end{aligned}$$

Applying inverse Elzaki transform

$$\begin{aligned} \mu(\psi, \phi, \varphi, \mathfrak{S}) &= E^{-1}\left[s^2 \mu(\psi, \phi, \varphi, 0) + s^\theta E\{\sin(\psi + 2\phi + 3\varphi) \cos \mathfrak{S}\}\right] \\ &+ E^{-1}\left[s^\theta E\{-3 \cos(\psi + 2\phi + 3\varphi) \sin \mathfrak{S}\}\right] - E^{-1}\left[s^\theta E\left\{\frac{\partial^3 \mu}{\partial \psi^3} + \frac{1}{8} \frac{\partial^3 \mu}{\partial \phi^3} + \frac{1}{27} \frac{\partial^3 \mu}{\partial \varphi^3}\right\}\right], \\ \mu_0(\psi, \phi, \varphi, \mathfrak{S}) &= E^{-1}\left[s^\theta E\left\{\sin(\psi + 2\phi + 3\varphi) \left(1 - \frac{\mathfrak{S}^2}{2!} + \frac{\mathfrak{S}^4}{4!} - \frac{\mathfrak{S}^6}{6!} + \frac{\mathfrak{S}^8}{8!}\right)\right\}\right]. \end{aligned}$$

Implementing the Adomian decomposition technique, we have

$$\begin{aligned} \sum_{j=0}^{\infty} \mu_j(\psi, \phi, \varphi, \mathfrak{S}) &= E^{-1}\left[s^\theta E\left\{-3 \cos(\psi + 2\phi + 3\varphi) \left(\mathfrak{S} - \frac{\mathfrak{S}^3}{3!} + \frac{\mathfrak{S}^5}{5!} - \frac{\mathfrak{S}^7}{7!} + \frac{\mathfrak{S}^9}{9!}\right)\right\}\right] \\ &- E^{-1}\left[s^\theta E\left\{\sum_{j=0}^{\infty} \frac{\partial^3 \mu_j}{\partial \psi^3} + \frac{1}{8} \sum_{j=0}^{\infty} \frac{\partial^3 \mu_j}{\partial \phi^3} + \frac{1}{27} \sum_{j=0}^{\infty} \frac{\partial^3 \mu_j}{\partial \varphi^3}\right\}\right], \\ \mu_0(\psi, \phi, \varphi, \mathfrak{S}) &= \sin(\psi + 2\phi + 3\varphi) \left(\frac{\mathfrak{S}^\theta}{\Gamma(\theta + 1)} - \frac{\mathfrak{S}^{\theta+2}}{\Gamma(\theta + 3)} + \frac{\mathfrak{S}^{\theta+4}}{\Gamma(\theta + 5)} - \frac{\mathfrak{S}^{\theta+6}}{\Gamma(\theta + 7)} + \frac{\mathfrak{S}^{\theta+8}}{\Gamma(\theta + 9)}\right), \tag{40} \\ \mu_1(\psi, \phi, \varphi, \mathfrak{S}) &= E^{-1}\left[s^\theta E\left\{-3 \cos(\psi + 2\phi + 3\varphi) \left(\mathfrak{S} - \frac{\mathfrak{S}^3}{3!} + \frac{\mathfrak{S}^5}{5!} - \frac{\mathfrak{S}^7}{7!} + \frac{\mathfrak{S}^9}{9!}\right)\right\}\right] \\ &- E^{-1}\left[s^\theta E\left\{\frac{\partial^3 \mu_0}{\partial \psi^3} + \frac{1}{8} \frac{\partial^3 \mu_0}{\partial \phi^3} + \frac{1}{27} \frac{\partial^3 \mu_0}{\partial \varphi^3}\right\}\right], \\ \mu_{j+1}(\psi, \phi, \varphi, \mathfrak{S}) &= -E^{-1}\left[s^\theta E\left\{\sum_{j=0}^{\infty} \frac{\partial^3 \mu_j}{\partial \psi^3} + \frac{1}{8} \sum_{j=0}^{\infty} \frac{\partial^3 \mu_j}{\partial \phi^3} + \frac{1}{27} \sum_{j=0}^{\infty} \frac{\partial^3 \mu_j}{\partial \varphi^3}\right\}\right], \end{aligned}$$

for  $j = 0, 1, 2, \dots$

$$\begin{aligned} \mu_1(\psi, \phi, \varphi, \mathfrak{S}) &= 0, \\ \mu_{j+1}(\psi, \phi, \varphi, \mathfrak{S}) &= 0. \end{aligned} \tag{41}$$

This readily yields the exact solution

$$\mu(\psi, \phi, \varphi, \mathfrak{S}) = \sin(\psi + 2\phi + 3\varphi) \left(\frac{\mathfrak{S}^\theta}{\Gamma(\theta + 1)} - \frac{\mathfrak{S}^{\theta+2}}{\Gamma(\theta + 3)} + \frac{\mathfrak{S}^{\theta+4}}{\Gamma(\theta + 5)} - \frac{\mathfrak{S}^{\theta+6}}{\Gamma(\theta + 7)} + \frac{\mathfrak{S}^{\theta+8}}{\Gamma(\theta + 9)}\right), \tag{42}$$

when  $\vartheta = 1$ , then EDM solution is

$$\mu(\psi, \phi, \varphi, \mathfrak{S}) = \sin(\psi + 2\phi + 3\varphi)\sin \mathfrak{S}. \quad (43)$$

Figure 7 consists of two plots the exact and EDM results of  $\mu(\psi, \mathfrak{S})$  of Example 4 at  $\vartheta = 1$ . Both the graphs of Figure 7 indicate that the current technique has close contact with the exact result for the given. In Figure 8, two plots are given that represent the approximate result of Example 4 at fractional  $\vartheta = 0.8$  and  $0.6$ , respectively. Figure 8 shows that the solution surfaces of the fractional-order are convergent to the integer-order surface as the fractional-order approaches to the integer-order. It suggests that through the physical phenomena happening in nature, we can model any of the surfaces as desire physically.

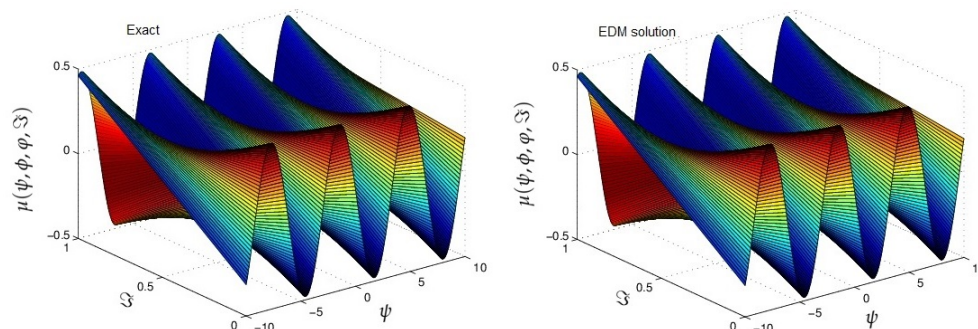


Figure 7. The graph of Exact and EDM solutions of  $\vartheta = 1$  of Example 4.

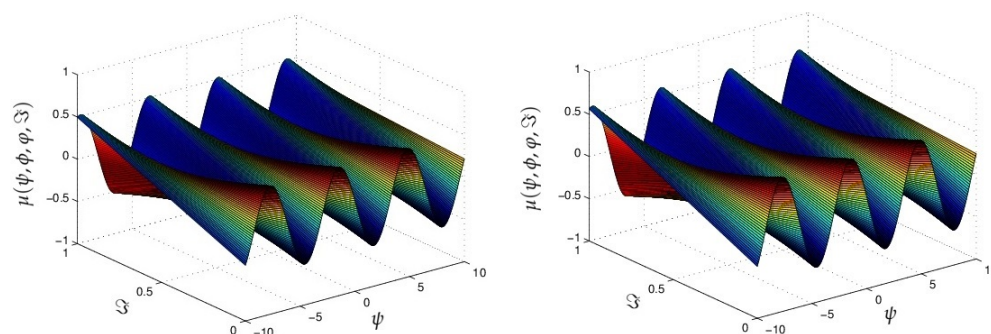


Figure 8. The graphs of different fractional-order  $\vartheta = 0.8$  and  $0.6$  of Example 4.

## 5. Conclusions

In this paper, the Elzaki decomposition method is implemented to obtain fractional-order multi-dimensional dispersive partial differential equations. The technique gives series form solutions that converge very quickly in actual solutions. It is predicted that the achieved results in this article will be helpful for further analysis of the complicated linear and nonlinear physical problems. The calculations of these techniques are very straightforward and simple. Thus, we deduce that this technique can be implemented to solve other fractional-order partial differential equations.

**Author Contributions:** The authors declare that this study was accomplished in collaboration with the same responsibility. All authors have read and agreed to the published version of the manuscript.

**Funding:** This research received no external funding.

**Institutional Review Board Statement:** Not applicable.

**Informed Consent Statement:** Not applicable.

**Data Availability Statement:** The numerical data used to support the findings of this study are included within the article.

**Acknowledgments:** This research was supported by Basic Science Research Program through the National Research Foundation of Korea (NRF) funded by the Ministry of Education (No. 2017R1D1A1B05030422).

**Conflicts of Interest:** The authors declare no conflict of interest.

## References

1. Miller, K.S.; Ross, B. *An Introduction to Fractional Calculus and Fractional Differential Equations*; Wiley: New York, NY, USA, 1993.
2. Kilbas, A.A.; Srivastava, H.M.; Trujillo, J.J. *Theory and Applications of Fractional Differential Equations*; Elsevier: Amsterdam, The Netherlands, 2006.
3. Podlubny, I. *Fractional Differential Equations*; Academic Press: New York, NY, USA, 1999.
4. Drapaca, C.S.; Sivaloganathan, S. A fractional model of continuum mechanics. *J. Elast.* **2012**, *107*, 105–123. [[CrossRef](#)]
5. Deshpande, A.; Daftardar-Gejji, V. Chaos in discrete fractional difference equations. *Pramana* **2016**, *87*, 1–10. [[CrossRef](#)]
6. Fang, L.; Liu, J.; Ju, S.; Zheng, F.; Dong, W.; Shen, M. Experimental and theoretical evidence of enhanced ferromagnetism in sonochemical synthesized BiFeO<sub>3</sub> nanoparticles. *Appl. Phys. Lett.* **2010**, *97*, 242501. [[CrossRef](#)]
7. Shah, N.A.; Dassios, I.; Chung, J.D. Numerical Investigation of Time-Fractional Equivalent Width Equations that Describe Hydromagnetic Waves. *Symmetry* **2021**, *13*, 418. [[CrossRef](#)]
8. Goswami, A.; Singh, J.; Kumar, D. Numerical simulation of fifth order Kdv equations occurring in magneto-acoustic waves. *Ain Shams Eng. J.* **2017**, *9*, 2265–2273. [[CrossRef](#)]
9. Steudel, H.; Drazin, P.G.; Johnson, R.S. *Solitons: An Introduction*, 2nd ed.; Cambridge Texts in Applied Mathematics; Cambridge University Press: Cambridge, UK, 1989.
10. Djidjeli, K.; Price, W.G.; Twizell, E.H.; Wang, Y. Numerical methods for the solution of the third-and fifth-order dispersive Korteweg-de Vries equations. *J. Comput. Appl. Math.* **1995**, *58*, 307–336. [[CrossRef](#)]
11. Zahran, M.A.; El-Shewy, E.K. Contribution of Higher-Order Dispersion to Nonlinear Electron-Acoustic Solitary Waves in a Relativistic Electron Beam Plasma System. *Phys. Scr.* **2007**, *6*, 803. [[CrossRef](#)]
12. Seadawy, A.R. New exact solutions for the KdV equation with higher order nonlinearity by using the variational method. *Comput. Math. Appl.* **2011**, *62*, 3741–3755. [[CrossRef](#)]
13. Shi, Y.; Xu, B.; Guo, Y. Numerical solution of Korteweg-de Vries-Burgers equation by the compact-type CIP method. *Adv. Differ. Equ.* **2015**, *2015*, 353. [[CrossRef](#)]
14. Yavuz, M.; Āzdemir, N. European vanilla option pricing model of fractional order without singular kernel. *Fractal Fract.* **2018**, *2*, 3. [[CrossRef](#)]
15. Thabet, H.; Kendre, S.; Chalishajar, D. New analytical technique for solving a system of nonlinear fractional partial differential equations. *Mathematics* **2017**, *5*, 47. [[CrossRef](#)]
16. Yepez-Martinez, H.; Gomez-Aguilar, F.; Sosa, I.O.; Reyes, J.M.; Torres-Jimenez, J. The Feng's first integral method applied to the nonlinear mKdV space-time fractional partial differential equation. *Rev. Mex. Fis.* **2016**, *62*, 310–316.
17. Prakash, A.; Kumar, M. Numerical method for fractional dispersive partial differential equations. *Commun. Numer. Anal.* **2017**, *1*, 1–18. [[CrossRef](#)]
18. Kocak, H.; Pinar, Z. On solutions of the fifth-order dispersive equations with porous medium type non-linearity. *Waves Random Complex Media* **2018**, *28*, 516–522. [[CrossRef](#)]
19. Kanth, A.R.; Aruna, K. Solution of fractional third-order dispersive partial differential equations. *Egypt. J. Basic Appl. Sci.* **2015**, *2*, 190–199.
20. Sultana, T.; Khan, A.; Khandelwal, P. A new non-polynomial spline method for solution of linear and non-linear third order dispersive equations. *Adv. Differ. Equ.* **2018**, *2018*, 316. [[CrossRef](#)]
21. Pandey, R.K.; Mishra, H.K. Homotopy analysis Sumudu transform method for time-fractional third order dispersive partial differential equation. *Adv. Comput. Math.* **2017**, *43*, 365–383. [[CrossRef](#)]
22. Adomian, G. *Solving Frontier Problems of Physics: The Decomposition Method*; With a Preface by Yves Cherruault; Fundamental Theories of Physics; Springer Science & Business Media: Berlin/Heidelberg, Germany, 1994; Volume 60.
23. Elzaki, T.M. The new integral transform Elzaki transform. *Glob. J. Pure Appl. Math.* **2011**, *7*, 57–64.
24. Elzaki, T.M. On the connections between Laplace and Elzaki transforms. *Adv. Theor. Appl. Math.* **2011**, *6*, 1–11.
25. Elzaki, T.M. On The New Integral Transform “Elzaki Transform” Fundamental Properties Investigations and Applications. *Glob. J. Math. Sci. Theory Pract.* **2012**, *4*, 1–13.
26. Jena, R.M.; Chakraverty, S. Solving time-fractional Navier-Stokes equations using homotopy perturbation Elzaki transform. *SN Appl. Sci.* **2019**, *1*, 16. [[CrossRef](#)]
27. Sedeeg, A.K.H. A coupling Elzaki transform and homotopy perturbation method for solving nonlinear fractional heat-like equations. *Am. J. Math. Comput. Model.* **2016**, *1*, 15–20.
28. Neamaty, A.; Agheli, B.; Darzi, R. Applications of homotopy perturbation method and Elzaki transform for solving nonlinear partial differential equations of fractional order. *J. Nonlinear Evol. Equ. Appl.* **2016**, *6*, 91–104.
29. Wazwaz, A.M. An analytic study on the third-order dispersive partial differential equations. *Appl. Math. Comput.* **2003**, *142*, 511–520. [[CrossRef](#)]